Journal of ELECTRICAL ENGINEERING, VOL. 59, NO. 6, 2008, 302–309

ANALYSIS AND CORRECTION OF CARRIER SPILLING EFFECT FOR DIFFERENT Si STRUCTURES

Marián Kuruc * — **Ladislav Hulényi** ** — **Rudolf Kinder** **

In this article we present a method for basic correction of carrier concentration profiles measured by the spreading resistance technique for the carrier spilling effect. It is shown how to calculate carrier distribution on the bevelled surface and what is the effect of the bevel on the distribution of free charge carriers. We also present how carrier spilling affects different silicon structures and whether the so-called zero field correction is sufficient. This is done on several typical silicon structures used in semiconductor technology. For comparison we used SIMS $N_{\mathrm{D}}(x)$ profiles and theoretical $N_{\mathrm{t}}(x)$ profiles simulated by DIOS.

K e y w o r d s: spreading resistance, carrier spilling, doping profile, carrier concentration profile, on-bevel profile, zero field correction, simulation, bevel

1 INTRODUCTION

In semiconductor industry, measurement of doping and carrier concentration profiles and determination of the junction depth are very important because the shape of the carrier concentration profile and the p-n junction depth determine the final electrical properties of semiconductor devices. For analysis of the doping concentration profiles the most frequently used methods are SIMS (Secondary Ion Mass Spectrometry), $N_{\mathrm{D}}(x)$ and Spreading Resistance Profiling (SRP) for measurement of carrier concentration profiles, $N_{\text{c-SRP}}(x)$. Alternatively, for calculation of the doping concentration profiles, $N_{\mathrm{t}}(x)$, process simulator SUPREM and ISE TCAD (Integrated System Engineering Technology Computer Aided Design containing code DIOS) are used. Especially, $N_{\text{c-SRP}}(x)$ profiles are important for electrical properties of semiconductor devices, that is why SRP method is very popular. However, it is important to understand that SRP profiles without correction for the so-called "carrier spilling effect" (CSE), which is a shift of the p-n junction at the surface of the semiconductor due to sample bevelling, represent only the on-bevel carrier concentration profile, $N_{\text{c-bevel}}(x)$. In certain cases this $N_{\text{c-bevel}}(x)$ profile can be different from the vertical carrier concentration profile $N_{\mathrm{c}}(x)$ in the unbevelled part of the measured sample. Therefore it is important to consider the influence of CSE on the $N_{\text{c-SRP}}(x)$ profiles measured by SRP when comparing to $N_{\mathrm{D}}(x)$ or $N_{\mathrm{t}}(x)$ profiles.

There are different approaches to correct $N_{\text{c-SRP}}(x)$ profile measured by the spreading resistance measurement technique for this effect. Some companies have developed their own software that basically use straightforward solutions of the Poisson equation in combination with dopant profiles obtained from a process simulator like SUPREM using multiple iterations to calculate the dopant profile which would result in measured on-bevel profile (the so-called SRP2 technique). Details of these techniques are described in [1, 2]. Other techniques use inverse solutions of the Poisson equation to reconstruct the dopant profile from the spreading resistance profile layer by layer [3, 4, 5, 6]. There was some research also done on the reduction of CSE by applying an appropriate external dc field between the probes and sample back that would counteract the intrinsic carrier spilling. This technique is referred to as a spreading impedance probe (SIP) [7].

We have developed a program that can calculate $N_{\text{c-bevel}}(x)$ profiles by combining process simulators such as SUPREM-IV (S4, Stanford University Process Engineering Models) or DIOS for calculating the doping profile $N_{\mathrm{t}}(x)$ and device simulator PISCES-2ET (Poisson and Continuity Equation Solver) for calculating the carrier concentration profile $N_{\mathrm{c}}(x)$. We also present an algorithm that is used to correct $N_{\text{c-SRP}}(x)$ profiles for carrier spilling using the zero-field (ZF) model correction. These corrections were then tested on different silicon structures and compared to $N_{\mathrm{t}}(x)$ profiles or $N_{\mathrm{D}}(x)$ profiles measured by SIMS, and sufficiency of ZF correction is analyzed.

2 THEORY

Spreading resistance profiling (SRP) is based on measuring the spreading resistance across the bevelled surface on the sample. In each point on the bevel, two specially conditioned probes are lowered onto the sample and the spreading resistance is measured using a low voltage (5 mV). This spreading resistance depth profile is then corrected for volume sampling effects using multilayer

* ON Semiconductor Slovakia, a.s., Vrbovská cesta 2617/102, 921 01 Piešťany, Slovakia; marian.kuruc@onsemi.com ** Slovak University of Technology, Faculty of Electrical Engineering, Department of Microelectronics, Ilkovičova 3, 812 19 Bratislava, Slovakia; ladislav.hulenyi@stuba.sk

ISSN 1335-3632

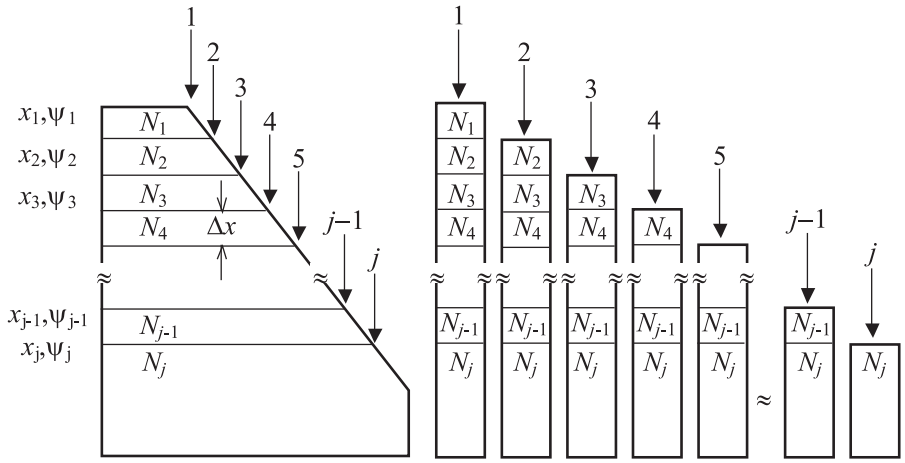

Fig. 1. Schematics of a multilayer structure approximation of a bevelled sample used for calculation of the $N_{\text{c-bevel}}(x)$ profile

correction algorithms and the concentration of charge carriers is calculated using calibration curves obtained on samples with known doping.

In some structures the electrically active dopant profile $N_{\text{D}}(x)$ is approximately equal to the net carrier concentration profile $N_{\text{c}}(x)$ derived from the experimental SRP data. This is true only if the space charge region is only a small fraction of the layer. For structures such as CMOS p- and n-wells, thin or lightly doped epitaxial layers and shallow source- drain layers a significant part of the layer contains non-zero space charge [8]. Conventional SRP data analysis of these structures is based on application of the Laplace equation, which assumes no net charge in the analyzed material. It is clear that spreading resistance profiles near a p-n junction or other significant resistivity inhomogeneity violate this assumption [1]. Therefore, the resulting carrier density profile presents only a poor estimation of electrically active dopant profile in submicrometer and lightly doped layers. This profile represents the so-called on-bevel carrier concentration $N_{\text{c-bevel}}(x)$ profile that is the concentration of charge carriers on the surface of the bevelled sample. This $N_{\text{c-bevel}}(x)$ profile can in some cases differ from the desired vertical carrier concentration profile $N_{\text{c}}(x)$. This difference is caused by removing a part of sample and, hereby, removing carriers by the process of bevelling. In 1986 Hu [9] showed by using the two-dimensional Poisson equation that carrier diffusion significantly distorted some spreading resistance profiles and the resulting junction depths appeared to be too shallow. For the same reason, implantation doses calculated from SRP data are often too small and calculated sheet resistance values are too large.

The $N(x)$ profile of the bevelled sample can be approximated by a multilayer structure consisting of a set of $j1$ thin layers with thickness Δx and constant doping N_i on top of a substrate with doping N_j. This structure is illustrated in Fig. 1.

Because of small angles used for sample preparation (usually less than 2°), 2D effects can be neglected and 1D approximation can be used. The $N_{\text{c}}(x)$ profile in the unbevelled structure is calculated from the $N_{\text{t}}(x)$ profile using the Poisson equation (1).

$$\frac{\mathrm{d}^2\psi(x)}{\mathrm{d}x^2} = -\frac{q}{\varepsilon_0\varepsilon_r}\left[N_D^-(x) - N_A^-(x) + p(\psi) - n(\psi)\right] \quad (1)$$

where ψ represents the local electrostatic potential, q is the elementary charge, ε_r is the relative permittivity, ε_0 is permittivity of vacuum, N_D^+ is the concentration of electrically active donors, N_A is the concentration of electrically active acceptors, p is the concentration of holes, n is the concentration of electrons. The carrier concentrations can be assumed to be near equilibrium because the applied voltages (on the measurement probes) are very small ($\sim$ 5 mV) and changes in minority carrier concentrations due to injection of carriers can be neglected [1]. The electron and hole concentrations must also satisfy equations (2) and (3)

$$n(\psi) = n_i \exp\left[\frac{q\psi(x)}{kT}\right] \quad (2)$$

$$p(\psi) = n_i \exp\left[-\frac{q\psi(x)}{kT}\right] \quad (3)$$

where n_i is the intrinsic carrier concentration, k is the Boltzmann constant and T is temperature. The charge carrier concentrations n and p are linked together by relation

$$np = n_i^2\,. \quad (4)$$

Potential ψ can be defined as a difference between the Fermi level E_f and the intrinsic Fermi level E_i

$$\psi = \frac{E_f - E_i}{q}\,. \quad (5)$$

For calculation of charge carrier concentrations n and p, equations (1), (2) and (3) have to be solved simultaneously for a given $N_{\text{t}}(x)$ profile [1]. For solving these

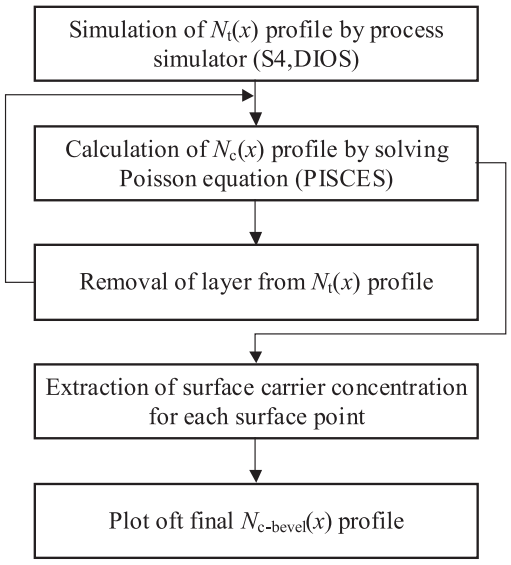

Fig. 2. Algorithm for calculation of $N_{\text{c-bevel}}(x)$ profile [10]

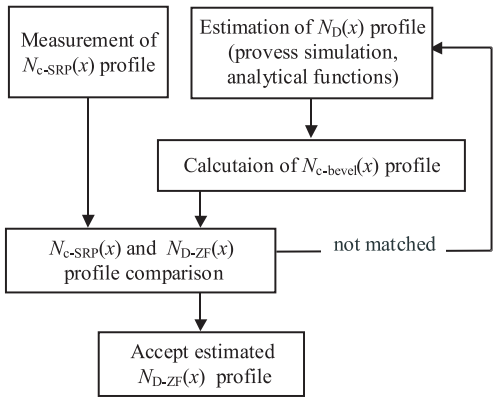

Fig. 3. Algorithm for calculation of assumed $N_{\text{D-ZF}}(x)$ profiles

equations the following boundary conditions are used. The first condition is that at the surface the electrical field is proportional to the surface charge Q_{ss}.

$$\left.\frac{\mathrm{d}\psi}{\mathrm{d}x}\right|_{x_i} = -\frac{Q_{ss}}{\varepsilon_0 \varepsilon_r} \tag{6}$$

and the second condition is that deep in the substrate the electrical field approaches zero and

$$\left.\frac{\mathrm{d}\psi}{\mathrm{d}x}\right|_{x} = 0\,. \tag{7}$$

In most analyses of carrier spilling, the surface charge is assumed to be zero or constant. Some authors assume a positive or negative surface charge Q_{ss} that generally can cause some further shift of the p-n junction [3]. The newest studies also report the influence of the probe pressure and penetration on this carrier spilling, referred to as pressure-enhanced carrier spilling [7]. In our experiments we used the zero surface charge model assuming the surface charge Q_{ss} equal to zero.

For simulation of $N_t(x)$ profiles we used programs S4 and DIOS. The vertical Nc(x) profile is calculated from $N_t(x)$ profile by solving the Poisson equation. This solution of the Poisson equation is achieved by device simulator PISCES-2ET. To calculate the $N_{\text{c-bevel}}(x)$ profile we used the algorithm shown in Fig. 2.

The algorithm shown in Fig. 2 is based on the process used in SRP2 technique [1] or its newer version EDP software for calculation of $N_{\text{c-bevel}}(x)$ profiles [8].

By using the forward solution of the Poisson equation and with the combination of process simulations (S4, DIOS) or analytical functions (Gaussian, error function, Pearson, exponential or step functions) it is possible to "correct"' the measured $N_{\text{c-SRP}}(x)$ profiles and to estimate the doping profile $N_{\text{D-ZF}}(x)$ that would result in the measured $N_{\text{c-SRP}}(x)$ profile. The algorithm for this type of "correction" is shown in Fig. 3 and is similar to the algorithm presented by Mazur [1] except that in this case we do not calculate the spreading resistance profile from the simulated doping profile and compare the spreading resistance profiles but we are comparing the carrier concentration profile measured by SRP with $N_{\text{c-bevel}}(x)$ calculated profile.

According to the algorithm in Fig. 2 and parameters from [1], a model for correction of the influence of CSE on the $N_{\text{c-SRP}}(x)$ profile was tested. First we simulate the technological process using process simulator to obtain $N_t(x)$ profile. Next, we calculate the carrier profile $N_c(x)$ using PISCES and extract the charge carrier concentration at the surface. Then we remove a layer from $N_t(x)$ profile and again calculate the $N_c(x)$ profile using PISCES and extract the charge carrier concentration at the surface. This is done till we have all points for reconstruction of the $N_{\text{c-bevel}}(x)$ profile. Then we plot these extracted surface points versus the depth they correspond to and obtain the $N_{\text{c-bevel}}(x)$ profile. This is the profile that is measured by the spreading resistance analysis. By comparing this with $N_c(x)$ profile on an unbevelled part of the sample we can see the impact of the carrier spilling effect on this profile. In Fig. 4 one can see an example of calculation of $N_{\text{c-bevel}}(x)$ profile for n-type implantation into lightly doped p-type substrate. The vertical $N_c(x)$ profile shows the concentration of free charge carriers in the unbevelled part of the sample and $N_{\text{c-bevel}}(x)$ profile shows the concentration of free charge carriers on the bevelled surface of the sample. The position of the metallurgical p-n junction (the depth where concentrations of donors and acceptors are equal) is located at depth $x_j = 2.35\,\mu$m ($N_t(x)$ profile). The position of the electrical p-n junction (the depth where concentrations of electrons and holes are equal) in the unbevelled part of the sample is at depth $x_j = 2.51\,\mu$m ($N_c(x)$ profile). On the calculated on-bevel profile, the depth of p-n junction is $x_j = 1.93\,\mu$m ($N_{\text{c-bevel}}(x)$ profile). As we can see in Fig. 3, the carrier spilling effect is responsible for a shift of the p-n junction from $x_j = 2.51\,\mu$m for vertical $N_c(x)$

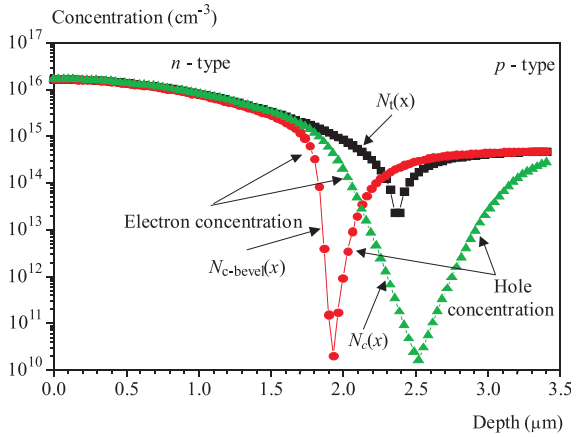

Fig. 4. Example of the influence of the carrier spilling effect on the Nc(x) profile for n-type implantation in a lightly doped p-type substrate

profile to $x_j = 1.93\,\mu$m for $N_{\text{c-bevel}}(x)$ profile. The p-n junction is shifted towards the surface by 580 nm that represents a 23 % shift of the p-n junction. Distribution of free charge carriers in the sample was simulated using 2D DIOS and is shown in Fig. 4. On this 2D plot of free charge carrier distributions you can see how removal of a part of the sample (and also of carriers) influences the distribution of carriers in the sample and the p-n junction is shifted towards the top of the sample.

3 EXPERIMENTAL

To analyze the effect of carrier spilling we used most common types of $N_c(x)$ profiles. We have made comparison with SIMS data and theoretical profiles simulated by DIOS. SIMS $N_{\text{D}}(x)$ profiles were measured by CAMECA 6F Magnetic Sector SIMS and the depth of the crater was measured by Tencor P10 Surface Profiler. Spreading resistance profiles were measured by the SSM2000 NanoSpreading Resistance Measurement system. Samples were bevelled using a 0.1 micron diamond paste. For measurement we used tungsten-osmium probes with a load of 10 grams, probe spacing 25 μm, probe contact diameter 3.3 μm and step $\Delta x = 3\,\mu$m. $N_{\text{c-bevel}}(x)$ profiles were calculated using the algorithm in Fig. 2 and calculation of $N_{\text{D-ZF}}(x)$ profiles (ZF correction) was done using algorithms in Figs. 2 and 3.

First we analyzed the epitaxial layer grown on the p-type substrate (boron, $6 \times 10^{14}\,\text{cm}^3$, crystallographic orientation $\langle 100 \rangle$). The epitaxial layer was n-type (arsenic, $5 \times 10^{15}\text{cm}^{-3}$) with layer thickness 6 μm. In Fig. 6 is shown the $N_{\text{c-SRP}}(x)$ profile measured by the spreading resistance profiling technique. Using algorithms shown in Figs. 2 and 3 we have reconstructed the expected $N_{\text{D-ZF}}(x)$ profile. This correction was made by finding the doping concentration profile ($N_{\text{d-ZF}}(x)$) that would result in the same on-bevel $N_{\text{c-bevel}}(x)$ profile as the $N_{\text{c-SRP}}(x)$ profile. This is the most commonly applied approach for correcting $N_{\text{c-SRP}}(x)$ profiles for CSE. Since for solving Poisson equations in algorithm in Fig. 2 we used the condition of zero surface charge, this correction is called the zero-field Poisson correction. For comparison there is also shown the $N_{\text{D}}(x)$ profile of arsenic measured by SIMS.

Next we focused on different types of p-type structures (different doses of boron and slopes of $N_{\text{c}}(x)$ profiles) in the same type and opposite type substrate. In Fig. 7 there is an example of p-type implantation (boron implantation, dose $N_{\text{d}} = 1.77 \times 10^{13}\text{cm}^2$) into lightly doped p-type substrate, crystallographic orientation $\langle 111 \rangle$. For comparison there are shown $N_{\text{c-SRP}}(x)$ profile, $N_{\text{D}}(x)$ measured by SIMS and $N\text{t}(x)$ profile simulated by DIOS. In Fig. 8, theoretically calculated on-bevel concentration of carriers ($N_{\text{c-bevel}}(x)$) are shown and also vertical carrier distribution $N_{\text{c}}(x)$ calculated from $N_{\text{t}}(x)$ profile.

Another similar structure is shown in Fig. 9. In this case it is a p-well structure (boron implantation, dose

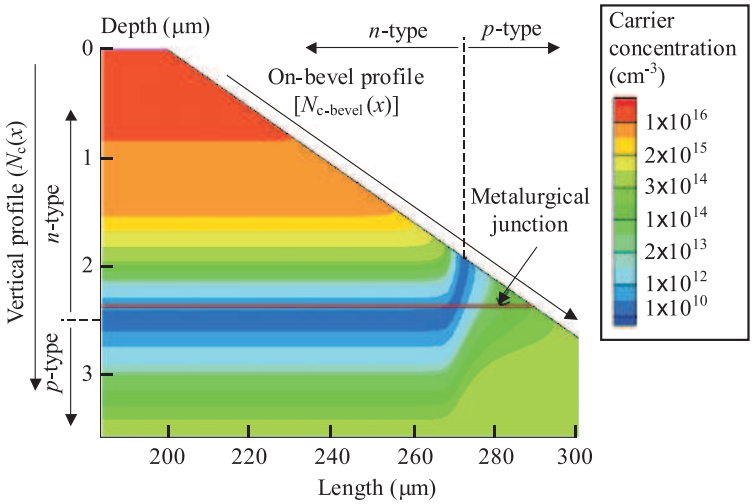

Fig. 5. Cross-section of the bevelled sample showing the change in the distribution of free charge carriers due to CSE for n-type implantation in a lightly doped p-type substrate

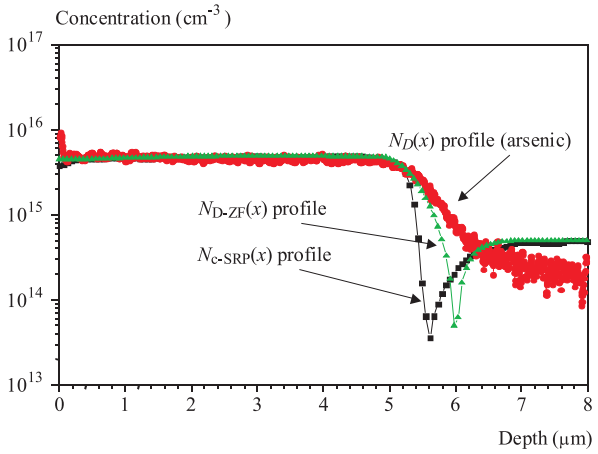

Fig. 6. Example of n-type epi layer in p-type substrate, comparison of $N_{\text{c-SRP}}(x)$, $N_{\text{D}}(x)$ and $N_{\text{D-ZF}}(x)$ profiles [11]

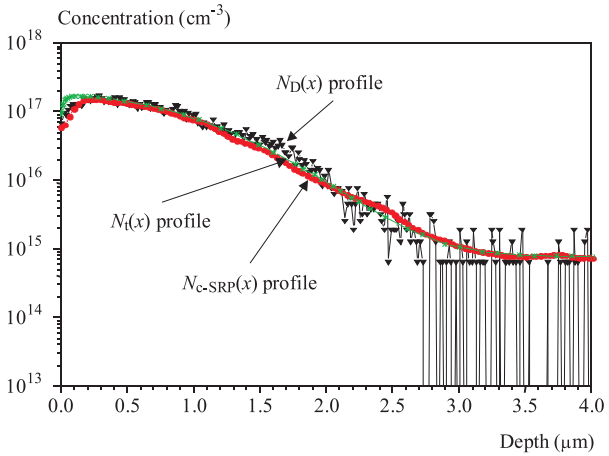

Fig. 7. Example of p-type implantation (boron implantation, dose $N_{\text{d}} = 1.77 \times 10^{13}\text{cm}^2$) into lightly doped p-type substrate, comparison of $N_{\text{c-SRP}}(x)$, $N_{\text{D}}(x)$ and $N_{\text{t}}(x)$ profiles

$N_{\text{d}} = 1.2 \times 10^{13}\text{cm}^2$) in a lightly doped p-type substrate. This sample has even lower doping than that in Fig. 7. Again, for comparison there are shown $N_{\text{c-SRP}}(x)$ profile, $N_{\text{D}}(x)$ measured by SIMS and $N_{\text{t}}(x)$ profile simulated by DIOS. Both of these structures were created by boron implantation into a boron doped substrate with crystallographic orientation $\langle 100 \rangle$.

Next we looked at p-type implantation into n-type substrate. A typical example of this type of profile is a p-type base structure (boron implantation, dose $N_{\text{d}} = 6.3 \times 10^{14}\text{cm}^2$) shown in Fig. 10. In this case we compare $N_{\text{c-SRP}}(x)$ profile, on-bevel $N_{\text{c-bevel}}(x)$ calculated (using algorithm in Fig. 2) from $N_{\text{t}}(x)$ profile simulated by DIOS profile as $N_{\text{c-SRP}}(x)$ profile. For reference there is also shown $N_{\text{D}}(x)$ profile of boron measured by SIMS.

Another comparison was made on a slightly different p-well structure (even lower dose and longer diffusion process than in Fig. 9) is shown in Fig. 11. Here we have prepared two samples, one sample was on substrate $\langle 100 \rangle$, p-type, and another sample was processed exactly in the same way except in this case we used a substrate with different conductivity $\langle 100 \rangle$, n-type. We have also made simulations for both structures and SIMS analysis for a sample with n-type substrate. For structure with n-type substrate we have also calculated $N_{\text{c-bevel}}(x)$ profile from $N_{\text{t}}(x)$ profile. All profiles are shown in Fig. 11.

Then we have focused on different types of n-type structures (different implantation doses and slopes of $N_{\text{c}}(x)$ profiles) in the same type and opposite type substrate. On Fig. 12 is shown typical buried collector structure created by heavy implantation (antimony implantation, dose $N_{\text{d}} = 5 \times 10^{15}\text{cm}^2$) followed by a long diffusion process. For comparison we have prepared same structures on both types of substrates and both profiles were corrected for carrier spilling effect using the algorithms shown in Figs. 2 and 3. For comparison we have also made simulations by process simulator DIOS ($N_{\text{t}}(x)$ profiles) using p-type substrate. Detailed view of profile region affected by carrier spilling is shown in Fig. 13.

In Fig. 14 there is an example of n-type implantation (phosphorus implantation, dose $N_{\text{d}} = 2.5 \times 10^{13}\text{cm}^2$) into lightly doped p-type substrate. For comparison there are shown $N_{\text{c-SRP}}(x)$ profile, corrected SRP profile $N_{\text{D-ZF}}(x)$, $N_{\text{D}}(x)$ profile measured by SIMS and $N_{\text{t}}(x)$ profile simulated by DIOS.

Another similar structure is shown on Fig. 15. In this case it is an n-well structure (phosphorus implantation, dose $N_{\text{d}} = 2 \times 10^{12}\text{cm}^{-2}$) in a lightly doped p-type substrate. Again for comparison there are shown $N_{\text{c-SRP}}(x)$ profile, corrected SRP profile $N_{\text{D-ZF}}(x)$, $N_{\text{D}}(x)$ measured by SIMS and $N_{\text{t}}(x)$ profile simulated by DIOS. All these structures (Figs. 12, 14 and 15) were created on substrates with crystallographic orientation $\langle 100 \rangle$.

4 DISCUSSION

In Fig. 6 the effect of CSE is shown on an n-type epitaxial layer grown on a p-type substrate. This is an example of a very steep profile in the junction area. The carrier spilling effect is responsible for shifting of the p-n junction by about $0.2\,\mu\text{m}$. Using algorithms in Figs. 2 and 3 we have reconstructed the expected $N_{\text{D-ZF}}(x)$ profile. When we compare the corrected $N_{\text{d-ZF}}(x)$ profile with SIMS $N_{\text{D}}(x)$ profile, we get excellent agreement between these two profiles. As can be seen for this type of profile correction, the use of ZF model seems to be sufficient and is able to recover $N_{\text{D}}(x)$ profile from $N_{\text{c-SRP}}(x)$ profile.

In Figs. 7 and 9 we can see p-type implantations into lightly doped p-type substrates (boron concentration in substrate $\langle 1 \times 10^{15}\text{cm}^3$). For both profiles we did not make any correction for the carrier spilling effect. However, when we compare measured the $N_{\text{c-SRP}}(x)$ profiles with either SIMS $N_{\text{D}}(x)$ profiles or DIOS simulated profiles $N_{\text{t}}(x)$, we can see good agreement between these profiles. The carrier spilling effect is present also in this case as shown in Fig. 8, however, it does not strongly affect the measured profile and the difference between $N_{\text{c-bevel}}(x)$ profile and $N_{\text{t}}(x)$ profile is very small. In this

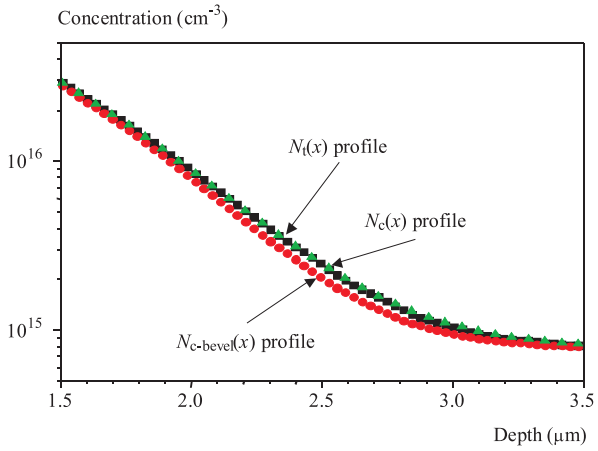

Fig. 8. Detailed view of theoretical $N_{0t}(x)$ profiles, calculated $N_c(x)$ and $N_{c\text{-bevel}}(x)$ profiles in the region influenced by carrier spilling, for the same structure as shown in Fig. 7

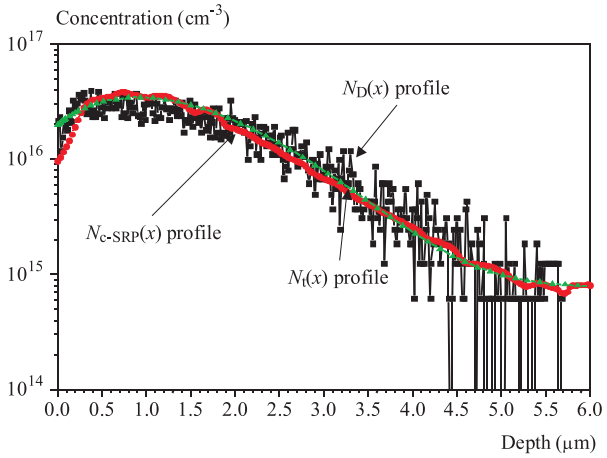

Fig. 9. Example of a p-well structure (boron implantation, dose $N_d = 1.2\times10^{13}\text{cm}^2$) in lightly doped p-type substrate, comparison of $N_{c\text{-SRP}}(x)$, $N_D(x)$ and $N_{D\text{-ZF}}(x)$ profiles

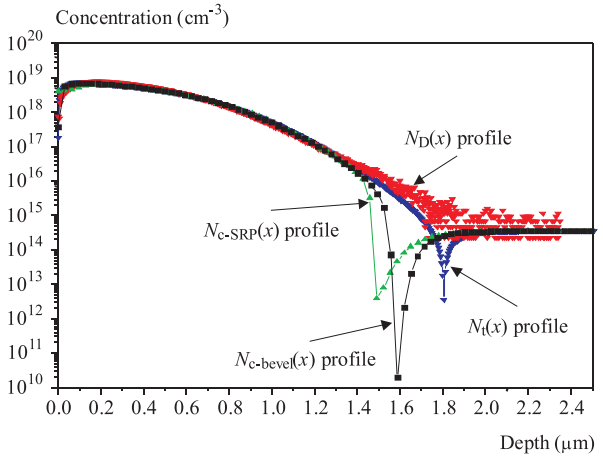

Fig. 10. Example of p-type base structure (boron implantation, dose $N_d = 6.3\times10^{14}\text{cm}^2$), comparison of $N_{c\text{-SRP}}(x)$, $N_D(x)$, $N_{c\text{-bevel}}(x)$ and $N_t(x)$ profiles

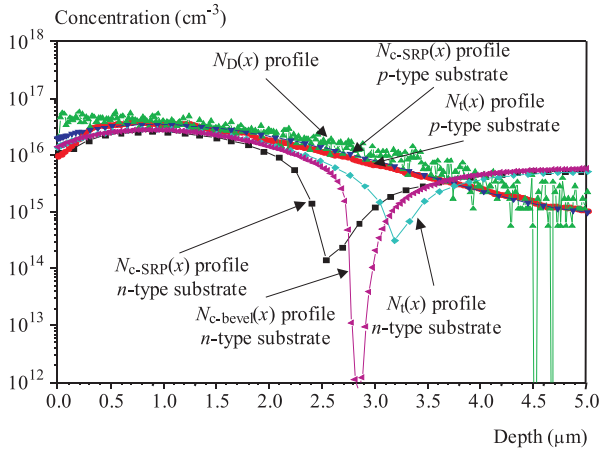

Fig. 11. Example of p-type boron implantation (p-well structure) in p-type and n-type substrate, comparison of $N_{c\text{-SRP}}(x)$, $N_D(x)$, $N_t(x)$ and $N_{c\text{-bevel}}(x)$ profiles for both types of substrate [11]

case the carrier spilling effect can be neglected without any significant error.

Situation becomes more complicated when we look at the profiles with p-n junctions. In Fig. 10 the base of a bipolar npn transistor is shown. In this case we compare $N_D(x)$ profile of boron measured by SIMS, $N_{c\text{-SRP}}(x)$ profile and $N_t(x)$ profile simulated by DIOS. From this $N_t(x)$ profile we calculated a theoretical on-bevel profile $N_{c\text{-bevel}}(x)$ using the algorithm in Fig. 2. From these profiles we can see that the difference between junction from $N_{c\text{-SRP}}(x)$ and $N_t(x)$ is about $0.35\,\mu\text{m}$. Using the zero-field correction we are able to explain most of the carrier spilling, and the difference between theoretical $N_{c\text{-bevel}}(x)$ profile and $N_{c\text{-SRP}}(x)$ profile is about $0.1\,\mu\text{m}$. As can be seen, ZF field model is able to explain most of the difference between $N_{c\text{-SRP}}(x)$ and $N_t(x)$ profiles however for some very shallow profiles this can be insufficient.

Most sensitive to the carrier spilling effect seem to be lightly doped slowly varying profiles that are usually used for p-well on n-well structures in twin well CMOS technology. A typical profile of p-well is shown in Fig. 11. In this case we prepared samples with different substrate types. It can be seen that for p-well in p-type substrate measured $N_{c\text{-SRP}}(x)$ profile, $N_D(x)$ profile and $N_t(x)$ profiles are almost the same (this has already been verified in Figs. 7 and 8. We can see that the carrier spilling is not visible or insignificant in this case, hence no correction is necessary. However, situation is dramatically different when we look at p-well in n-type substrate. In this case we have used $N_t(x)$ profile calculated by DIOS simulation as a reference and used our algorithm for calculation of on-bevel $N_{c\text{-bevel}}(x)$ profile. When we compare the measured $N_{c\text{-SRP}}(x)$ profile and calculated on-bevel profile, we can see that there is still a significant difference in the junction depth ($0.3\,\mu\text{m}$). When we consider that the theoretical $N_t(x)$ profile matches with the measured $N_D(x)$ SIMS profile, we can say that for this type of profiles ZF correction is insufficient and is not able to fully correct the measured profiles. ZF mode is able to explain only 50 % of the junction shift. In this case other factors like pressure enhanced carrier spilling, Schottky

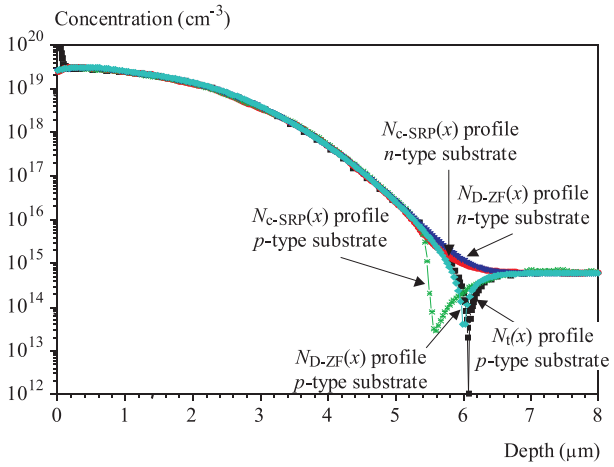

Fig. 12. Example of n-type buried collector structure in p-type and n-type substrate, comparison of $N_{\text{c-SRP}}(x)$, $N_{\text{D-ZF}}(x)$ profiles for both types of substrate and $N_{\text{t}}(x)$ profile for p-type substrate

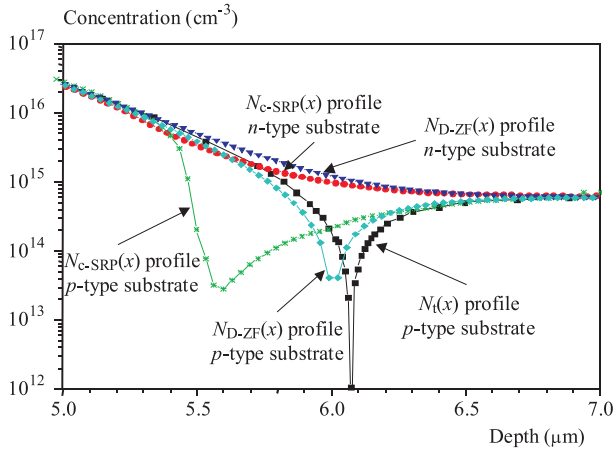

Fig. 13. Example of n-type buried collector structure in p-type and n-type substrate, comparison of $N_{\text{c-SRP}}(x)$, $N_{\text{D-ZF}}(x)$ profiles for both types of substrate and $N_{\text{t}}(x)$ profile for p-type substrate

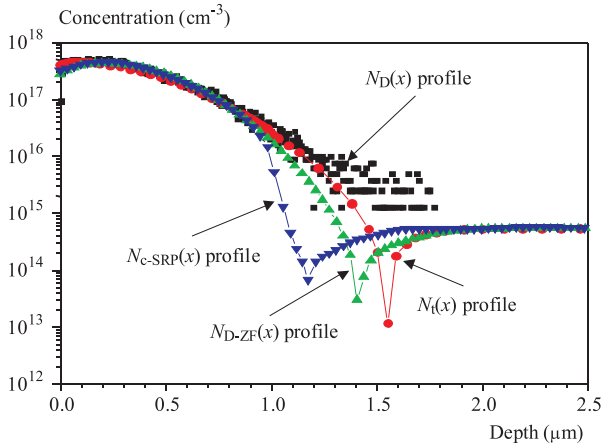

Fig. 14. Example of n-type medium dose implantation in p-type substrate, comparison of $N_{\text{c-SRP}}(x)$, $N_{\text{D}}(x)$, $N_{\text{t}}(x)$ and $N_{\text{D-ZF}}(x)$ profiles

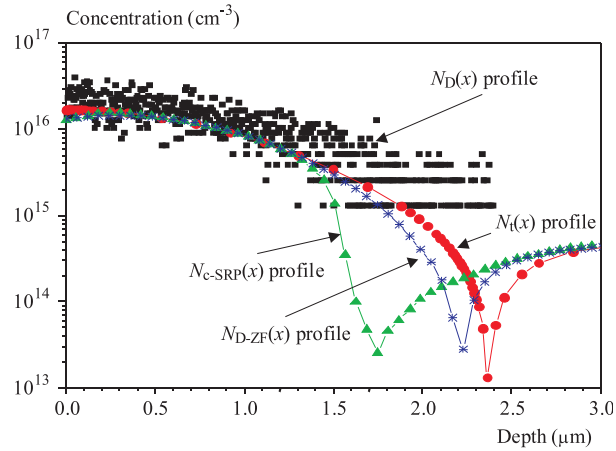

Fig. 15. Example of n-type phosphorus implantation (n-well structure) in p-type substrate, comparison of $N_{\text{c-SRP}}(x)$, $N_{\text{D}}(x)$, $N_{\text{t}}(x)$ and $N_{\text{D-ZF}}(x)$ profiles

effects and surface states related distortions [6] start to play important role and need to be accounted for.

As a next typical profile we have looked at a buried collector structure used in bipolar devices to reduce the collector resistance. It is a structure created by high dose implantation ($> 1 \times 10^{15}\text{cm}^2$, antimony or arsenic). We have prepared this structure on both types of substrates and it is shown in Fig. 12 and a detailed view of the junction area is shown in Fig. 13. For comparison there is also shown a theoretical $N_{\text{t}}(x)$ profile simulated by DIOS. In this case we have made correction for carrier spilling for $N_{\text{c-SRP}}(x)$ profiles for both substrates. As can be seen, again there is a small effect of carrier spilling for $N_{\text{c-SRP}}(x)$ profile in the n-type substrate. When we compare the corrected ND-ZF(x) profile with $N_{\text{t}}(x)$ profile, we get very good agreement between these profiles with difference of junction depths $< 0.1\,\mu$m. For these types of profiles ZF correction seems to be sufficient. There can also be seen excellent agreement between $N_{\text{D-ZF}}(x)$ profiles for both substrates.

The structure shown in Fig. 14 is medium dose implantation ($N_{\text{d}} = 1.5 \times 10^{13}\text{cm}^2$). In this case we compare $N_{\text{c-SRP}}(x)$ and $N_{\text{D-ZF}}(x)$ profile with $N_{\text{D}}(x)$ SIMS profile and $N_{\text{t}}(x)$ profile. As we can see difference between $N_{\text{D-ZF}}(x)$ profile and $N_{\text{t}}(x)$ profile is $0.15\,\mu$m. The difference in the junction depth for $N_{\text{c-SRP}}(x)$ and $N_{\text{t}}(x)$ profile is $0.37\,\mu$m, however, ZF model can explain only a shift of $0.22\,\mu$m. In this case this model is insufficient and other factors need to be incorporated into correction to fully recover the $N_{\text{D}}(x)$ profile.

A similar situation for n-well structure is shown in Fig. 15. In this case the carrier spilling effect is responsible for shifting the p-n junction by about $0.64\,\mu$m towards the surface ($N_{\text{c-SRP}}(x)$ profile vs. $N_{\text{t}}(x)$ profile). Using ZF correction we are able to explain $0.49\,\mu$m shift that presents a significant part of the difference (76 %) and there still remains a difference about $0.15\,\mu$m that is not accounted for using this correction. When we compare these results with p-well structure, which is shown in Fig. 11, we can see that for p-type structures in n-type substrate there is more additional carrier spilling compared to n-type structures in p-type substrate.

The next analyzed structure was n-well in p-type substrate (Fig. 3). This is a similar type like in Fig. 2, but

with opposite conductivities. As one can see, the carrier spilling effect is responsible for shifting of p-n junction by about $0.5\,\mu$m. In this case the carrier spilling correction seems to be very near the measured SIMS profile and the junction depths determined from $N_{\mathrm{D}}(x)$ profile and $N_{\mathrm{D\text{-}ZF}}(x)$ profile are very similar. From this we can conclude that ZF correction seems to be sufficient. From these data we can see that p-type structures in n-type substrate are more influenced by additional carrier spilling than n-type in p-type. For p-well in n-type substrate the ZF model was able to explain only 50 % of junction shift but for n-well structures we were able to explain only 76 % of the difference. This is in agreement with other authors [6] that also claim the carrier spilling effect to be more pronounced for p-type structures in n-type substrates.

5 CONCLUSION

We have developed and tested a program for calculation of carrier distribution on a bevelled surface $N_{\mathrm{c\text{-}bevel}}(x)$ profile and for comparing the of $N_{\mathrm{c\text{-}SRP}}(x)$ profile measured by SRP with simulated $N_{\mathrm{t}}(x)$ profiles. We have also successfully made the so-called zero-field correction of different $N_{\mathrm{c\text{-}SRP}}(x)$ profiles using algorithms in Figs. 2 and 3 and analyzed the carrier spilling effect for different Si structures. We have made 2D simulation how the distribution of charge carriers is influenced by the bevelling process (Figs. 4 and 5), and hereby visualized the carrier spilling effect.

To analyze the influence of CSE we used different samples, where we compared $N_{\mathrm{c\text{-}SRP}}(x)$ profiles and corrected profiles $N_{\mathrm{D\text{-}ZF}}(x)$ with SIMS $N_{\mathrm{D}}(x)$ profiles, theoretical $N_{\mathrm{t}}(x)$ profiles and $N_{\mathrm{c\text{-}bevel}}(x)$ profiles. We have shown that CSE has a very small effect on the structures without p-n junction (Figs. 7, 8, 9, 11, 12, 13) and in some cases can be neglected. For steep profiles, like an n-type epitaxial layer on p-type substrate, ZF correction is able to fully recover $N_{\mathrm{D}}(x)$ profile (Fig. 6). Also for other steeper profiles as shown in Figs. 10 and 12, ZF model is able to almost fully correct the profile for this effect. However, for slowly varying lightly doped profiles the ZF model is insufficient and is not able to fully correct $N_{\mathrm{c\text{-}SRP}}(x)$ profiles (Figs. 11, 14, 15). Especially for p-well structure in n-type substrate ZF model it was able to recover only 50 % of difference (Fig. 11) and this type of structure is extremely affected by additional CSE. This is why it is necessary to make further corrections for such effects like the probe pressure, Schottky effects and surface states to fully explain the difference.

Acknowledgements

This work was done in Center of Excellence CENAMOST (Slovak Research and Development Agency Contract. No. VVCE-0049-07) with support of grants of the Slovak Grant Agency Vega No. 1/3111/06, and APVV-20-055405.

References

[1] MAZUR, R. G.: J. Vac. Sci. Technol. B **10**(1) (Jan/Feb 1992), 397.

[2] PAWLIK, M.: J. Vac. Sci. Technol. B **10**(1) (Jan/Feb 1992), 388.

[3] DICKEY, D. H.: J. Vac. Sci. Technol. B **10**(1) (Jan/Feb 1992), 438.

[4] LEONG, M. S.—CHOO, S. C.—LEE, Y. T.—ONG, H. L.—NG, K. P.: J. Vac. Sci. Technol. B **10**(1) (Jan/Feb 1992), 426.

[5] CLARYSSE, T.—EYBEN, P.—DUHAUON, N.—XU, M. W.—VANDERWORST, W.: J. Vac. Sci. Technol. B **21**(2) (Mar/Apr 2003), 729.

[6] CLARYSSE, T.—VANHAEREN, V.—HOFLIJK, I.—VANDERWORST, W.: Characterization of Electrically Active Dopant Profiles with the Spreading Resistance Probe, Materials Science & Engineering **47** No. 5-6 (31 Dec 2004).

[7] CZECH, I.—CLARYSSE, T.—VANDERWORST, W.: J. Vac. Sci. Technol. B **12**(1) (Jan/Feb 1994), 298.

[8] Electrically Active Dopant Profiler (EDP) for SRP, Application Brief, Solid State Measurements, Inc., rev.1.0, (Feb 2004).

[9] HU, S. M.: J. Appl. Phys. **53** (1982), 1499.

[10] KURUC, M.—HULENYI, L.—KINDER, R.: Simulation of Carrier Spilling Effect for Bevelled Structures, In: Proceedings of the 12$^{\mathrm{th}}$ international workshop on Applied Physics of Condensed Matter, APCOM 2006, Malá Lučivná, Slovakia, ISBN 80-227-2424-6, June 21-23, (2006), 92.

[11] KURUC, M.—HULENYI, L.—KINDER, R.: Analysis of Carrier Spilling Effect for Different Si Structures, In: Proceedings of the 14$^{\mathrm{th}}$ international workshop on Applied Physics of Condensed Matter, APCOM 2007, Malá Lučivná, Slovakia, ISBN 80-227-2424-6, June 27-29, (2007), 92.

Received 21 August 2007

Marián Kuruc (Ing) was born in Piešťany in 1979. He graduated in microelectronics from the Faculty of Electrical Engineering and Information Technology, Slovak Technical University, Bratislava. Since 2004 he worked as a defectivitty engineer in ON Semiconductor Slovakia and process integration engineer in the same company. His activities are oriented towards epitaxy, diffusion and implantation process characterizations in semiconductors using measurements and simulations.

Ladislav Hulenyi (doc, Ing, CSc) was born in Senica n/Myjavou in 1938. Graduated from the Faculty of Electrical Engineering, Slovak Technical University, Bratislava, in radiotechnology in 1962 and gained the CSc (PhD) degree in Electronics and Vacuum Technology at the same university, in 1976. Since 1979 has has worked as Assoc. Professor at the Department of Microelectronics, Faculty of Electrical Engineering and Information Technology. His research activity has been focused on the properties of semiconductor structures and devices.

Rudolf Kinder (doc, Ing, CSc) was born in Pezinok in 1940. He worked in electrotechnical industry in Bratislava. Then he worked at VURUP (Research Center for Petrol Chemistry) in the field of automation of chemical services. He graduated in technical cybernetics from the Faculty of Electrical Engineering, Slovak Technical University, Bratislava. He received CSc (PhD) degree in electronics and vacuum technology in 1984. He has worked as a senior scientist since 1989. Since 1996 he has been Associate Professor in microelectronics. His research activities are oriented towards semiconductor technology, particularly to analysis and simulation.